A mega-analysis of low frequency resting-state measures in psychosis-spectrum and mood disorders

Maya L. Foster[1], Milana Khaitova[2], Saloni Mehta[2], Jean Ye[3], Dustin Scheinost[1-6]

1) Department of Biomedical Engineering, Yale University
2) Department of Radiology & Biomedical Imaging, Yale School of Medicine
3) Interdepartmental Neuroscience Program, Yale School of Medicine
4) Department of Statistics & Data Science, Yale University
5) Child Study Center, Yale School of Medicine
6) Yale Biomedical Imaging Institute, Yale School of Medicine

Highest Academic Degrees Obtained by Co-Authors:

- Maya L. Foster – M.S./M.Phil.
- Milana Khaitova – B.A.
- Saloni Mehta – M.B.B.S.
- Jean Ye – M.S.
- Dustin Scheinost – Ph.D.

All correspondence and offprint requests should be sent or mailed to Maya L. Foster (maya.foster@yale.edu), Magnetic Resonance Research Center (MRRC), 300 Cedar St, New Haven, CT 06519.

Key Points

Question: How do the amplitude and complexity of low-frequency oscillation in fMRI signals associate with transdiagnostic psychosis-spectrum and mood disorders?

Findings: Findings suggest that the amplitude and complexity of low-frequency oscillation is associated with mental health in wide-spread and global manner. Complexity, which is well-studied in EEG but not fMRI—emerged as a promising measure for further research. Our results also support a frequency-based behavioral encoding system operating in the BOLD signal.

Meaning: Our findings show that psychosis-spectrum and mood disorders differ from healthy controls and each other in a whole-brain, but mechanistically distinct way. These transdiagnostic markers may form common disruptions that disorder-specific deviations can build on and may help in developing treatment strategies that target shared disruptions.

ABSTRACT

Objective: Conduct a mega-analysis of two complementary measures of resting-state functional magnetic resonance imaging (rsfMRI) dynamics—amplitude of low-frequency fluctuation (ALFF) and low-frequency spectral entropy (lfSE)—in a transdiagnostic mood and psychosis-spectrum sample to evaluate group differences and clinical symptom associations.

Design: ALFF and lfSE were calculated at the node-level by filtering data from 0.01 Hz to 0.08 Hz, regressing demographic variables, and harmonizing sites. Group differences were assessed using the Wilcoxon signed test. Symptom associations were evaluated with Spearman's rho. Analyses were conducted at both whole-brain and network levels, with sensitivity analyses to evaluate the impact of frequency brands.

Setting: Four open-source case-control datasets with resting-state functional magnetic resonance imaging were used: the Center for Biomedical Research Excellence, the Human Connectome Project for Early Psychosis, the Strategic Research Program for Brain Sciences, and the UCLA Consortium for Neuropsychiatric Phenomics.

Participants: Included participants had a mood disorder (bipolar, dysthymia, or major depressive disorder, n=228, aged 38.31 ± 12.56 years), a psychosis-spectrum disorder (early psychosis or schizophrenia spectrum disorder, n=318, aged 29.8 ± 13.21 years), or a healthy control (n=535, aged 39.89 ± 15.3 years).

Main outcomes and Measures: To identify transdiagnostic group differences and to evaluate mood and psychosis symptom associations using ALFF and lfSE.

Results: ALFF in psychosis-spectrum was significantly lower than mood disorders and controls (q's<0.001) at the whole-brain and network levels. lfSE in controls was significantly lower than both psychosis-spectrum and mood disorders at the whole-brain and network levels (q's<0.001). Whole-brain ALFF is positively associated with mood symptoms (rho=0.27, p<0.05). Whole-brain lfSE is negatively associated with positive (rho=-0.13, p<0.05) and mood (rho=-0.38, p<0.01) symptoms. Across frequency analyses, mood disorders exhibited greater sensitivity to group differences and symptom associations.

Conclusions and Relevance: Widespread, global differences in ALFF and lfSE underly transdiagnostic spectra of psychosis-spectrum and mood disorders. lfSE may be applicable for wider use in fMRI. Spectral measures of brain dynamics may represent transdiagnostic markers of mental health.

INTRODUCTION

Modern approaches treat psychiatric disorders on a spectrum that encompasses symptoms of varying severities[1–5]. Psychosis-spectrum (e.g., early psychosis and schizophrenia) and mood disorders (e.g., major depressive disorder and bipolar disorder) are examples of disorders that can exist on a spectrum[6] and cause significant disability globally[7–10] (Ayano et al., 2021; Sekhon & Gupta, 2023; Calabrese & Al Khalili, 2023). Cases of co-occurrence are also very common for these disorders. As such, the diagnoses likely share some biological mechanisms[6,11,12].

Mega-analyses are a promising approach for finding shared biological indices across disorders. These analyses pool neuroimaging data from several smaller studies to maximize population variance, increase generalizability, and improve statistical power by producing larger effect sizes[13,14] (Costafreda et al., 2009; Bigdely-Shamlo et al., 2020). By better accounting for psychiatric heterogeneity, mega-analyses analyses can also support the development of treatments that target shared clinical mechanisms of multiple conditions[2,15,16] (McQuaid, 2021, Holmes and Patrick, 2018; Zambrano-Vazquez et al., 2017).

Brain dynamics are widely associated with cognition and mental health[17–20] (Newson et al., 2019, Raut et al., 2021, Xu et al., 2023, Foster et al., 2024). Spectral measures succinctly characterize these dynamics across frequency bands[21–23] (Duff et al., 2008, Elble and Ondo, 2022, Zang et al., 2022) and are ideal for mega-analyses. They are computationally tractable in large samples, easy to pool across diverse datasets due to their conceptual simplicity, and neurobiologically interpretable at different spatial scales (i.e., regional, network, or whole brain levels). One widely used

metric is the amplitude of low-frequency fluctuations (ALFF), which quantifies the signal strength in the 0.01-0.08 Hz range and is well-established in functional neuroimaging[24–27] (Zou et al., 2008, Yang et al., 2007, Zuo et al., 2010, Li et al., 2021, Yen et al., 2023). A complementary measure is low-frequency spectral entropy (lfSE)—a frequency-bounded derivative of spectral entropy that quantifies the complexity or unpredictability of fMRI signal fluctuations in the 0.01–0.08 Hz range. Spectral entropy has been broadly used in EEG[28], but not fMRI.

ALFF and lfSE provide distinct, but complementary insights (amplitude versus complexity) into intrinsic brain dynamics that may help biologically differentiate disorders and mediate individual differences in symptom severity. Prior work has identified ALFF differences across major functional networks in psychosis-spectrum[29–32] (Turner et al., 2013; Wang et al., 2019, Li et al., 2023; Chen et al., 2024) and mood disorders[33,34,32] (Chen et al., 2024; Wang et al., 2012). In schizophrenia, studies found reduced ALFF in default mode, salience, sensorimotor, parietal, and visual networks compared to healthy controls[35] (Gong et al., 2020). Early-stage schizophrenia has been marked by increased ALFF in subcortical and visual networks and decreased ALFF in default mode and parietal networks[35] (Gong et al., 2020). In contrast, chronic schizophrenia includes widespread increases in ALFF across frontal, salience, temporal, and limbic networks, alongside reductions in sensorimotor, parietal, and occipital areas[35] (Gong et al., 2020). In depression, studies report increased ALFF in several regions—including lateralized subcortical areas, occipital lobe, limbic areas, frontoparietal network, and the default mode network—compared to matched healthy controls[34,36–39] (Wu et al., 2021, Chen et al., 2022, Zhang et al., 2021, Zhang et al., 2022, Luo et al., 2025). Decreased ALFF is

also observed in somatosensory cortex[33,40,36] (Wu et al., 2021), limbic areas (Liu et al., 2013, Wang et al., PLOS, 2012), and cerebellum[41,42] (Liu et al., 2014, Zhou et al., 2017) for major depressive disorder (MDD) compared to controls. In bipolar disorder, increased ALFF in the right caudate and putamen[43], bilateral insula, medial prefrontal cortex, and decreased ALFF in the left cerebellum[44] have been observed. In contrast, lfSE has not been studied in mood and psychosis populations.

Here, we perform a mega-analysis in over 1000 individuals to compare ALFF and lfSE in psychosis-spectrum and mood disorders to healthy controls. Our study expands on previous empirical findings by adding a complexity measure (i.e., lfSE)[45] (Tenev et al., 2025), using a large-scale sample size (n=1081), and comparing measures across a wider range of symptoms. We also assess the clinical significance of the measures by testing their association with relevant symptom measures. We hypothesized that ALFF and lfSE group differences will be in the frontoparietal[46,47] (Menon et al., 2011; Foster et al., 2025), salience[46] (Menon et al., 2011), and default mode networks[46,48] (Menon et al., 2011, Schilbach et al., 2016).

147 **METHODS**

148 **Participants.** We used four publicly available resting-state fMRI datasets (see Table
149 1 for participant demographics), the Center for Biomedical Research Excellence[49]
150 (COBRE), the Human Connectome Project Early Psychosis[50] (HCP-EP), the Strategic
151 Research Program for Brain Sciences[51] (SRPBS) Multi-disorder Connectivity Dataset,
152 and the University of California Los Angeles (UCLA) Consortium for Neuropsychiatric
153 Phenomics[52] (CNP). The COBRE dataset participants were recruited from the
154 University of New Mexico Psychiatric Center and the Raymond G. Murphy Veterans
155 Affairs Medical Center. This sample included 58 controls, and 41 patients diagnosed
156 with schizophrenia or schizoaffective disorder between 18 and 64 years of age. The
157 HCP-EP quality-controlled dataset consisted of 112 early psychosis (EP) patients
158 (within the first five years of the first presentation of psychosis symptoms) and 57
159 healthy controls (HCs) aged 16-35 from four different recruitment sites: Beth Israel
160 Deaconess Medical Center, McLean Hospital, and Massachusetts General Hospital,
161 and Indiana University). The sample also includes affective and non-affective psychosis
162 patients diagnosed according to the DSM-V[53]. Affective patients had a mood disorder
163 with psychosis diagnosis (e.g., major depression with psychosis or bipolar disorder with
164 psychosis)[52]. The SRPBS dataset is a transdiagnostic population of patients with mood
165 and psychosis symptoms of varying severities. The final sample included HCs (n=281),
166 individuals diagnosed with schizophrenia spectrum disorder (SSD, n=124), and
167 individuals diagnosed with a mood spectrum disorder (n=182; bipolar with unknown
168 subtype=46, dysthymia=2, and major depressive disorder=134) aged 16-80 from 7
169 different recruitment sites in Japan: Center of Innovation at Hiroshima University (COI),

170 Hiroshima Kajikawa Hospital (HKH), Hiroshima Rehabilitation Center (HRC), Hiroshima
171 University Hospital (HUH), Kyoto University (KUT), Showa University (SWA), and
172 University of Tokyo Hospital (UTO). Participants in all datasets underwent resting-state
173 functional magnetic resonance imaging (rsfMRI). The CNP quality-controlled sample
174 has 117 healthy individuals, 41 schizophrenia, and 46 bipolar disorder (subtype
175 unknown) participants from the local community aged 21-50.
176
177 **Symptom Measures**. For psychosis symptoms, the Positive and Negative Syndrome
178 Scale[54] (PANSS) was used and assesses the presence and severity of positive,
179 negative, and general psychopathology within the past week in individuals with
180 psychosis-spectrum disorder. The scale is widely used in clinical psychosis studies and
181 has demonstrated reliability in assessing psychopathology across patient populations. A
182 subset of the HCP-EP (n=107) and SRPBS (n=123) datasets had the PANSS (n=230).
183 The Beck's Depression Inventory[55] (BDI-II) was used to assess the symptom burden in
184 individuals with mood disorders and health controls. The BDI-II measures hallmark
185 symptoms of depression and has high internal consistency[55,56]. Subset of the SRPBS
186 dataset had the BDI-II (total n=62; controls n=23; mood disorder n=39)
187
188 **Data Preprocessing.** The acquisition and imaging parameters for the datasets are
189 detailed elsewhere[49,50,57,51]. However, an abridged version is available in the
190 Supplement (see Table S1). Images were motion and slice time corrected using
191 SPM12[58] (Shen et al. 2013). BioImage Suite was used to perform mean white matter
192 regression, cerebral spinal fluid regression, and gray matter time, removing linear

trends, and low-pass filtering[59]. The Shen-268 atlas[58] was warped from Montreal Neurological Institute (MNI) space into single-subject space. Next, the mean-time course of each node was calculated by averaging its constituent voxels' time-series data.

Quality Control. Participants were excluded if they had an average frame-to-frame displacement exceeding 0.2 mm **(**n=28), insufficient quality of linear or nonlinear registration (n=16), had >100 missing nodes (n=10) or had less than 75% coverage of relevant nodes for a given network or whole-brain analysis (n=15, see Supplement for more details on data preservation process). This left a final sample of 1081 subjects for further analysis: 823 for whole-brain analyses (averaging across all nodes) and varying sample sizes for network analyses (Table S2-3).

ALFF Calculation and Analysis. First, the power spectral density of each node's time series was calculated using periodogram function from the SciPy [60] signal processing API in Python 3.9. This calculation entailed converting each participant's node time-series into the frequency domain via the fast Fourier transform (FFT). Then, the power spectral density was integrated over the low-frequency range (0.01 Hz ≤ frequency ≤ 0.08 Hz) using SciPy's trapezoid integration method to calculate total power. Next, we took the square root of that operation to quantify ALFF.

$$\mathrm{ALFF} = \sqrt{\int_{f=0.01\,Hz}^{0.08\,Hz} P(f)\mathrm{df}}$$

Note: f=frequency and df=delta frequency

ALFF in this study is considered a proxy for the intensity of neural-associated brain activity or the energy content of the low-frequency band. A high ALFF signifies greater oscillation intensity while a low ALFF signifies lower oscillation intensity in the low-frequency range. ALFF was assessed group-wise at the whole-brain by averaging all nodes and network-levels using 10 canonical networks from the Shen 268 atlas.

Low-frequency Spectral Entropy Calculation and Analysis. lfSE was also calculated at the node-level. Individual node time-series underwent a band-pass filter in the low-frequency range (0.01 Hz ≤ frequency ≤ 0.08 Hz) using SciPy's butter and filtfilt functions (order = 2)[24]. The signal was transformed into the frequency domain using FFT, followed by power spectral density calculation and normalization to a probability density function. Then, lfSE was calculated as the Shannon entropy of the power spectral density was calculated using AntroPy[61] package in Python 3.

$$\hat{S}_{spectral} = \frac{-\sum_{f=0}^{Fs/2} P(f)\log_2 P(f)}{\log_2(num_f)}, \quad 0.01\,Hz < f < 0.08\,Hz$$

Note: f=frequency, Fs=sampling frequency, num_f= number of frequencies derived by the FFT

As a complexity measure, high lfSE (flatter power spectral density spectrum) represents low complexity while low lfSE (power spectral density distribution with more peaks) represents high complexity. lfSE was assessed group-wise at the whole-brain by averaging all nodes and network-levels using 10 canonical networks from the Shen 268 atlas.

Statistical Analyses. Statistical analyses were constrained to the whole-brain and

network levels to capture macroscale brain. Additionally, broader scale analyses (i.e., network level) have greater power than granular level of inference[62]. Group comparisons of each low-frequency brain measure were evaluated at $p<0.05$ using the Wilcoxon two-sided rank sum test while correcting for multiple comparisons with false discovery rate (FDR). We controlled for several variables of non-interest: self-reported age, motion, and sex. First, these factors were regressed[63] using a generalized linear model on ALFF and lfSE values at the node level. Second, we applied the ComBat[64] R package to harmonize data across sites. For empirical ranges, please refer to table S5). Where relevant, we report corrected (q) and uncorrected (p) results for transparency but only interpret significant corrected results ($q<0.05$).

Secondary analyses. We correlated symptoms scores (PANSS and BDI-II) and covariate-regressed ALFF and lfSE values using Spearman's correlation at the whole-brain and network levels. Participants for the PANSS analyses came from multiple sites and underwent site harmonization using ComBat[65]. Participants for the BDI-II analyses came from one site, so harmonization was not applied. Network-level associations were considered statistically significant at $q<0.05$ after FDR correction. Additionally, we evaluated similarity between the ALFF and lfSE by correlating these values across participants ($p<0.05$) using Spearman's rho at the whole-brain and network levels.

We also performed and compared two one-sided Wilcoxon and t-tests in both directions (group 1 < group 2, group 2 < group 1, etc.) to assess if the directionality of significant difference effects converged. For example, if network A had significant difference maps between psychosis-spectrum and mood disorder for ALFF and lfSE,

then the group averaged node-wise maps for both measures underwent two-one sided sample t-tests and two Wilcoxon one-tailed signed rank tests. The significant directionalities between the measures with both statistical tests would be compared.

Sensitivity Analysis. To assess the robustness of our findings, we used different frequency cutoffs (0.01-0.045 Hz and 0.035-0.09 Hz) to assess if finer spectral divisions were driving the identified trends and associations[66].

RESULTS

Participant clinical characteristics and demographics. Included participants (n = 1081) consisted of n = 513 HCs (COBRE=58, HCP-EP = 57, SRPBS = 279, UCLA=117), n = 318 psychosis-spectrum (COBRE=41, HCP-EP=112, SRPBS=124, UCLA=41), and n=214 mood disorder participants (SRPBS=168). Demographics, symptom scores, and diagnosis breakdowns of included subjects (n=1081) are summarized in Table 1 and S4. Significant group differences were found for self-reported sex (χ^2=18.081, df = 2, p<0.001), age (W=75.48, df=2, p<0.001), and average frame displacement (W= 8.599, df=2, p=0.014). The age of psychosis-spectrum participants (29.8 ± 13.21 years) was significantly lower than mood disorders (38.31 ± 12.56) and controls (39.89 ± 15.3 years). Participants with mood disorders also had significantly higher motion frame displacement (0.087 ± 0.045 mm) compared to matched healthy controls (0.083 ± 0.046 mm) and those with psychosis-spectrum disorder (0.075 ± 0.037. (F=3.31; df=1, p<0.01).

Group differences in ALFF. At the whole-brain level, mood disorders exhibited the greatest ALFF, followed by controls and then psychosis-spectrum (Figure 2A, S2). Psychosis-spectrum ALFF values were significantly lower than both mood disorders and controls (p's<0.001). No differences in whole-brain ALFF were detected between mood disorders and controls. Similar differences were observed at the network level, where all networks showed significant (q's<0.05, FDR-corrected) differences when comparing psychosis-spectrum to mood disorders or health controls (Table 2). Results were similar when potential outliers were removed (Table S6) and when removing psychosis-

spectrum patients with known affective disorders (Table S7).

Group differences in lfSE. At the whole-brain level, psychosis-spectrum showed the highest lfSE, followed by mood disorders and then healthy controls (Figure 2B). Controls were significantly lower than both psychosis-spectrum and mood disorders at the whole-brain (p's<0.001). No differences in whole-brain lfSE were detected between psychosis-spectrum and mood disorders. At the network level, all networks exhibited significant differences between health controls and psychosis-spectrum (q's<0.05, FDR-corrected). The medial frontal, frontoparietal, motor, subcortical, and cerebellar networks exhibited significant differences between health controls and mood disorders (q's<0.05, FDR-corrected). Surprisingly, while no differences between psychosis-spectrum and mood disorders existed at the whole-brain level, every network (other than the cerebellar network) exhibited significant between-group differences (q's<0.05, FDR-corrected), likely due to the increases sample size used in the network analyses (Table 3). Results were similar when removing psychosis-spectrum patients with known affective disorders (Table S8).

The distribution of lfSE in psychosis-spectrum was bimodal. As this second peak in the distribution may influence results, we repeated analyses after removing it and potential high leverage points (see Supplemental Methods, Figure S4). Afterwards, results were similar (Tables S9). However, mood disorders (not psychosis-spectrum) showed the highest lfSE, and only visual networks remained significantly different between psychosis-spectrum and mood disorders (q's<0.05, FDR-corrected).

Associations with psychosis and mood symptoms. Whole-brain ALFF is positively associated with BDI-II scores (rho=0.27, p= 0.0355; Figure 2C, Table S10) but had no association with PANSS scores (Table S11). Additionally, whole-brain lfSE is negatively associated with positive PANSS (rho=-0.13, p=0.0418, Table S12) and BDI-II scores (rho=-0.38, p=0.002; see Figure 2D-E, Table S13). No other significant associations with ALFF or lfSE at the whole-brain or network-level were observed (Tables S10-13).

Correlation of ALFF and lfSE. At all scales of analysis, ALFF and lfSE were negatively correlated, such that individuals with higher ALFF values had lower lfSE values (Table S14). This relationship was also observed in our group comparison, where ALFF was consistently greater in mood disorder compared to psychosis-spectrum across scales and lfSE was consistently greater in psychosis-spectrum compared to mood disorder across scales.

Sensitivity analyses of finer-scale frequency ranges. Results at the finer-scale frequency ranges were broadly like main results with wide-spread differences observed between groups (Tables S15-22). However, results involving the mood disorder group exhibited the most changes when moving to finer-scale frequency ranges. For example, the lfSE of the DMN was significantly different between controls and mood disorders at 0.035-0.090 Hz, but not 0.01-0.045 Hz or the full frequency range. Additionally, whole-brain ALFF was positively associated with BDI-II scores at 0.01-0.045 Hz but negatively associated at 0.035-0.09 Hz (Table S18).

DISCUSSION

We investigated two spectral measures that capture complementary dimensions of brain dynamics—oscillation intensity and complexity—in psychosis-spectrum and mood disorders through a mega-analysis of resting-state fMRI. Our results strongly support that spectral measures of brain dynamics may represent transdiagnostic markers of mental health.

Notably, ALFF and lfSE differentiated clinical groups in unique ways, providing distinct insights into the biological underpinnings of mood and psychosis disorders. Across whole-brain and network analyses, mood disorders on average had higher amplitude oscillations than psychosis-spectrum disorders, whereas for complexity, this trend was reversed. Additionally, mood symptoms may be connected to various changes in brain dynamics, as reflected by significant associations with both ALFF and lfSE. For both measures, psychosis-spectrum exhibited larger, widespread differences compared to mood disorders and controls[67,68], while mood disorder lfSE exhibited more focal differences compared to controls[69]. In contrast to several studies [33,34,36–42], we did not observe case-control differences for mood disorder ALFF. These studies focused on single diagnoses and a finer spatial scale of analysis, which would yield specific spatial results that could be averaged out in a transdiagnostic approach like ours.

We also observed that our initial band (0.01-0.08 Hz) masked many significant effects in mood disorder ALFF and lfSE. Larger group differences and significant associations with mood symptoms were revealed in the narrower 0.035-0.090 Hz frequency band. Moreover, there was a reversal in the sign of significant associations with mood symptoms in the two finer-scale frequency bands (0.01-0.045 Hz and 0.035-

355 0.090 Hz). Aligned with these findings, a previous study showed that associations
356 between depressive symptoms and spectral measures in the subgenual gyrus differ
357 between frequency bands[70]. These diverging associations are evidence of the functional
358 specificity of frequency bands in the blood-oxygen level dependent (BOLD) signal[71–73].
359 Indeed, different frequency bands have been thought to reflect physiology occurring at
360 different intrinsic time scales[74–76]. In other words, specific frequency ranges have unique
361 functional relevance. As such, the finer bands may comprise multiple physiological
362 processes that contribute to mood disorder pathology. If too broad a frequency range is
363 adopted, interactive effects[70] can dominate and obscure significant results in a
364 competitive or mutually constructive way[77]. Continued investigations of the functional
365 relevance of specific frequency bands in mood disorders, as well as other psychiatric
366 conditions are needed.

367 Despite our initial hypotheses, there is widespread overlap in the functional
368 networks that had significant case-control differences in signal complexity for mood and
369 psychosis-spectrum disorders. These findings are consistent with a developing
370 consensus that psychiatric disorders generally affect similar systems[11]. This shared
371 spatial vulnerability can also explain the frequent co-occurrence of mood and psychosis-
372 spectrum disorders[6,78].

373 Several significant findings at the whole-brain level across measures and groups
374 suggest that mental health is a global phenomenon. The broader literature also
375 supports this, reporting a wide range of regions and networks functionally altered in
376 mood disorders[79] and psychosis-spectrum[80]. This global effect may also reflect the
377 transdiagnostic nature of our study. Treating patients on a spectrum can identify the

common denominators across diagnoses, which likely span broader circuits than disorder-specific effects. Under this consideration, how the system is affected at a regional or voxel level is what determines disorder specificity. As these common effects are established, future work can investigate how disorder-specific, and even individual-specific, deviations lead to unique symptom profiles[81].

In general, lfSE outperformed ALFF in detecting significant group differences and symptom associations. We hypothesize that this is because lfSE more effectively captures changes in brain dynamics and state transitions. As a measure of complexity and irregularity[82], it considers the entire energy distribution across a frequency band. Additionally, lfSE was the only measure linked to positive symptoms of psychosis. Previous work employing similar methods in other imaging modalities have identified signal irregularity and high signal variance as key features of the psychosis-spectrum[83–86]. Our results, alongside these findings from the broader literature, collectively position lfSE—a standard measure in the EEG literature[28] and related modalities[82,87–89] —as a valuable biologically-based index for broader application in fMRI.

This study has several strengths. We used transdiagnostic samples of participants, which may better reflect the dimensional nature of disorders and allows datasets with different diagnostic criteria to be combined in a mega-analysis. We also included two spectral measures, including lfSE (which is uncommon in fMRI analysis). It also has several limitations. First, participants were assumed to exclusively have a mood or psychosis disorder. Given comorbidities in these populations, it is unlikely that participants exclusively had a mood or psychosis disorder. However, this approach also better captures real-world phenotypes, where comorbidities are common[90]. Second, we

focus on measures that compress brain dynamics into a single number. More complex summaries of dynamic measures[91] may prove to be more sensitive and is a natural next step. Third, although we identify associations with symptoms scores, causality cannot be established. Lastly, transdiagnostic approaches can obscure disorder-specific differences that are not shared across all disorders.

Through a transdiagnostic mega-analysis, we investigated group differences in spectral measures of brain dynamics in psychosis and mood disorders. By combining distinct diagnoses into broader spectrums, we prioritized detecting commonalities, which can explain disorder co-occurrence. Nevertheless, our approach revealed distinct brain signal properties in addition to shared characteristics between the two patient groups. Future studies should continue to elucidate common denominators as well as diagnosis-, symptom-, and individual-specific brain deviations that build on top of disorder commonalities. Better characterization of shared brain features, and disorder specific deviations could pave the way towards plausible prevention and tailored treatment efforts.

Data and Code Availability

Data are publicly available through the Center for Biomedical Research Excellence Phase I grant[49], the Human Connectome Project Early Psychosis[50], the Strategic Research Program for Brain Sciences[51] and the UCLA Consortium for Neuropsychiatric Phenomics LA5c Study[52] (https://openneuro.org/datasets/ds000030/versions/00016). Preprocessing scripts are available at https://www.nitrc.org/projects/bioimagesuite.

Acknowledgements. We are grateful to the participants who dedicated their time and energy to participate in these large-scale data consortiums as well as the study team who collected and collated the data.

Funding Support. This publication was made possible by CTSA Grant Number UL1 TR001863 from the National Center for Advancing Translational Science (NCATS), a component of the National Institutes of Health (NIH). Its contents are solely the responsibility of the authors and do not necessarily represent the official views of NIH. This work was also supported by NIH grants R01MH126133-03 (to MF), F31AA032179 (to JY), R01MH121095 (to DS and SM), and 5R01DK136623-02 (to DS and MK).

Author Contributions and Assistive Grammar Tools Acknowledgement. MF had full access to the data and takes on full responsibility for accuracy of the data analysis. MF conceived and designed the study. MF participated in the acquisition, preprocessing, analysis, and interpretation of data. MF and DS participated in drafting the manuscript. MF and DS performed statistical analyses. SM provided critical review

of the content and provided clinical interpretations of the analyses. MK participated in quality control of data. JY participated in acquisition and preprocessing of some of the data.

Portions of the writing in this manuscript were edited with artificial intelligence (AI)-based tools to improve clarity and grammar. The authors critically reviewed and edited all AI-assisted content to ensure accuracy and originality. No AI tools were used in the generation of scientific content, data analysis, or interpretation. All intellectual content, interpretations, and conclusions are our own.

Study concept and design: Foster, Scheinost.
Acquisition, analysis, or interpretation of data: All authors.
Drafting of the manuscript: Foster, Scheinost.
Critical revision of the manuscript for important intellectual content: All authors.
Statistical analysis: Foster, Scheinost.
Obtained funding: Scheinost.
Administrative, technical, or material support: All authors.
Study supervision: Scheinost.

Conflict of Interest Disclosures. All authors reported receiving grants from the National Institutes of Health during the study. No other disclosures were reported.

Role of the Funder/Sponsor: Funding sources had no role in the study design,

collection, management, analysis, and interpretation of the data; preparation, review, or approval of the manuscript; and decision to submit the manuscript for publication.

REFERENCES

1. Insel T, Cuthbert B, Garvey M, et al. Research domain criteria (RDoC): toward a new classification framework for research on mental disorders. *Am J Psychiatry*. 2010;167(7):748-751. doi:10.1176/appi.ajp.2010.09091379

2. Zambrano-Vazquez L, Levy HC, Belleau EL, et al. Using the research domain criteria framework to track domains of change in comorbid PTSD and SUD. *Psychol Trauma*. 2017;9(6):679-687. doi:10.1037/tra0000257

3. Shah JL, Scott J, McGorry PD, et al. Transdiagnostic clinical staging in youth mental health: a first international consensus statement. *World Psychiatry*. 2020;19(2):233-242. doi:10.1002/wps.20745

4. Cuthbert BN. Research Domain Criteria (RDoC): Progress and Potential. *Curr Dir Psychol Sci*. 2022;31(2):107-114. doi:10.1177/09637214211051363

5. Wise T, Robinson OJ, Gillan CM. Identifying Transdiagnostic Mechanisms in Mental Health Using Computational Factor Modeling. *Biological Psychiatry*. 2023;93(8):690-703. doi:10.1016/j.biopsych.2022.09.034

6. Mood and psychotic disorders. Nature. December 21, 2023. Accessed August 11, 2025. https://www.nature.com/collections/chccdehgji

7. Ayano G, Demelash S, yohannes Z, et al. Misdiagnosis, detection rate, and associated factors of severe psychiatric disorders in specialized psychiatry centers in Ethiopia. *Ann Gen Psychiatry*. 2021;20:10. doi:10.1186/s12991-021-00333-7

8. Calabrese J, Al Khalili Y. Psychosis. In: *StatPearls*. StatPearls Publishing; 2024. Accessed March 31, 2024. http://www.ncbi.nlm.nih.gov/books/NBK546579/

9. Sekhon S, Gupta V. Mood Disorder. In: *StatPearls*. StatPearls Publishing; 2025. Accessed February 14, 2025. http://www.ncbi.nlm.nih.gov/books/NBK558911/

10. Global, regional, and national burden of 12 mental disorders in 204 countries and territories, 1990–2019: a systematic analysis for the Global Burden of Disease Study 2019. *The Lancet Psychiatry*. 2022;9(2):137-150. doi:10.1016/S2215-0366(21)00395-3

11. Xie C, Xiang S, Shen C, et al. A shared neural basis underlying psychiatric comorbidity. *Nat Med*. 2023;29(5):1232-1242. doi:10.1038/s41591-023-02317-4

12. Fusar-Poli P, Solmi M, Brondino N, et al. Transdiagnostic psychiatry: a systematic review. *World Psychiatry*. 2019;18(2):192-207. doi:10.1002/wps.20631

13. Costafreda SG. Pooling fMRI data: meta-analysis, mega-analysis and multi-center studies. *Front Neuroinform*. 2009;3. doi:10.3389/neuro.11.033.2009

14. Bigdely-Shamlo N, Touryan J, Ojeda A, Kothe C, Mullen T, Robbins K. Automated EEG mega-analysis I: Spectral and amplitude characteristics across studies. *NeuroImage*. 2020;207:116361. doi:10.1016/j.neuroimage.2019.116361

15. McQuaid RJ. Transdiagnostic biomarker approaches to mental health disorders: Consideration of symptom complexity, comorbidity and context. *Brain Behav Immun Health*. 2021;16:100303. doi:10.1016/j.bbih.2021.100303

16. Holmes AJ, Patrick LM. The Myth of Optimality in Clinical Neuroscience. *Trends in Cognitive Sciences*. 2018;22(3):241-257. doi:10.1016/j.tics.2017.12.006

17. Newson JJ, Thiagarajan TC. EEG Frequency Bands in Psychiatric Disorders: A Review of Resting State Studies. *Front Hum Neurosci*. 2019;12. doi:10.3389/fnhum.2018.00521

18. Raut RV, Snyder AZ, Mitra A, et al. Global waves synchronize the brain's functional systems with fluctuating arousal. *Sci Adv*. 2021;7(30):eabf2709. doi:10.1126/sciadv.abf2709

19. Xu Y, Long X, Feng J, Gong P. Interacting spiral wave patterns underlie complex brain dynamics and are related to cognitive processing. *Nat Hum Behav*. 2023;7(7):1196-1215. doi:10.1038/s41562-023-01626-5

20. Foster M, Scheinost D. Brain states as wave-like motifs. *Trends in Cognitive Sciences*. Published online 2024. Accessed April 29, 2024. https://www.cell.com/trends/cognitive-sciences/abstract/S1364-6613(24)00057-3

21. Duff EP, Johnston LA, Xiong J, Fox PT, Mareels I, Egan GF. The power of spectral density analysis for mapping endogenous BOLD signal fluctuations. *Human Brain Mapping*. 2008;29(7):778-790. doi:10.1002/hbm.20601

22. Elble RJ, Ondo W. Tremor rating scales and laboratory tools for assessing tremor. *J Neurol Sci*. 2022;435:120202. doi:10.1016/j.jns.2022.120202

23. Zang Z, Qiao Y, Yan S, Lu J. Reliability and Validity of Power Spectrum Slope (PSS): A Metric for Measuring Resting-State Functional Magnetic Resonance Imaging Activity of Single Voxels. *Front Neurosci*. 2022;16:871609. doi:10.3389/fnins.2022.871609

24. Zou QH, Zhu CZ, Yang Y, et al. An improved approach to detection of amplitude of low-frequency fluctuation (ALFF) for resting-state fMRI: Fractional ALFF. *Journal of Neuroscience Methods*. 2008;172(1):137-141. doi:10.1016/j.jneumeth.2008.04.012

25. Yang H, Long XY, Yang Y, et al. Amplitude of low frequency fluctuation within visual areas revealed by resting-state functional MRI. *Neuroimage*. 2007;36(1):144-152. doi:10.1016/j.neuroimage.2007.01.054

26. Zuo XN, Di Martino A, Kelly C, et al. The Oscillating Brain: Complex and Reliable. *Neuroimage*. 2010;49(2):1432-1445. doi:10.1016/j.neuroimage.2009.09.037

27. Li MT, Zhang SX, Li X, et al. Amplitude of Low-Frequency Fluctuation in Multiple Frequency Bands in Tension-Type Headache Patients: A Resting-State Functional Magnetic Resonance Imaging Study. *Front Neurosci*. 2021;15. doi:10.3389/fnins.2021.742973

28. Yen C, Lin CL, Chiang MC. Exploring the Frontiers of Neuroimaging: A Review of Recent Advances in Understanding Brain Functioning and Disorders. *Life*. 2023;13(7):1472. doi:10.3390/life13071472

29. Turner JA, Damaraju E, Van Erp TGM, et al. A multi-site resting state fMRI study on the amplitude of low frequency fluctuations in schizophrenia. *Front Neurosci*. 2013;7. doi:10.3389/fnins.2013.00137

30. Li X, Liu Q, Chen Z, et al. Abnormalities of Regional Brain Activity in Patients With Schizophrenia: A Longitudinal Resting-State fMRI Study. *Schizophrenia Bulletin*. 2023;49(5):1336-1344. doi:10.1093/schbul/sbad054

31. Wang P, Yang J, Yin Z, et al. Amplitude of low-frequency fluctuation (ALFF) may be associated with cognitive impairment in schizophrenia: a correlation study. *BMC Psychiatry*. 2019;19:30. doi:10.1186/s12888-018-1992-4

32. Chen C, Zhang B, Qin X, et al. Altered resting-state brain activity of the superior parietal cortex and striatum in major depressive disorder and schizophrenia. *Asian Journal of Psychiatry*. 2024;102:104303. doi:10.1016/j.ajp.2024.104303

33. Wang L, Dai W, Su Y, et al. Amplitude of Low-Frequency Oscillations in First-Episode, Treatment-Naive Patients with Major Depressive Disorder: A Resting-State Functional MRI Study. *PLOS ONE*. 2012;7(10):e48658. doi:10.1371/journal.pone.0048658

34. Chen Q, Bi Y, Zhao X, et al. Regional amplitude abnormities in the major depressive disorder: A resting-state fMRI study and support vector machine analysis. *Journal of Affective Disorders*. 2022;308:1-9. doi:10.1016/j.jad.2022.03.079

35. Gong J, Wang J, Luo X, et al. Abnormalities of intrinsic regional brain activity in first-episode and chronic schizophrenia: a meta-analysis of resting-state functional MRI. *J Psychiatry Neurosci*. 2020;45(1):55-68. doi:10.1503/jpn.180245

36. Wu Z, Luo Q, Wu H, et al. Amplitude of Low-Frequency Oscillations in Major Depressive Disorder With Childhood Trauma. *Front Psychiatry*. 2021;11:596337. doi:10.3389/fpsyt.2020.596337

37. Zhang B, Qi S, Liu S, Liu X, Wei X, Ming D. Altered spontaneous neural activity in the precuneus, middle and superior frontal gyri, and hippocampus in college

569 students with subclinical depression. *BMC Psychiatry*. 2021;21(1):280.
570 doi:10.1186/s12888-021-03292-1

571 38. Zhang Z, Bo Q, Li F, et al. Increased ALFF and functional connectivity of the right
572 striatum in bipolar disorder patients. *Progress in Neuro-Psychopharmacology and*
573 *Biological Psychiatry*. 2021;111:110140. doi:10.1016/j.pnpbp.2020.110140

574 39. Luo G, Zhou J, Liu L, Song X, Peng M, Zhang X. Abnormal ReHo and ALFF values
575 in drug-naïve depressed patients with suicidal ideation or attempts: Evidence from
576 the REST-meta-MDD consortium. *Progress in Neuro-Psychopharmacology and*
577 *Biological Psychiatry*. 2025;136:111210. doi:10.1016/j.pnpbp.2024.111210

578 40. Liu F, Guo W, Liu L, et al. Abnormal amplitude low-frequency oscillations in
579 medication-naive, first-episode patients with major depressive disorder: a resting-
580 state fMRI study. *J Affect Disord*. 2013;146(3):401-406.
581 doi:10.1016/j.jad.2012.10.001

582 41. Liu J, Ren L, Womer FY, et al. Alterations in amplitude of low frequency fluctuation
583 in treatment-naïve major depressive disorder measured with resting-state fMRI.
584 *Human Brain Mapping*. 2014;35(10):4979-4988. doi:10.1002/hbm.22526

585 42. Zhou M, Hu X, Lu L, et al. Intrinsic cerebral activity at resting state in adults with
586 major depressive disorder: A meta-analysis. *Progress in Neuro-*
587 *Psychopharmacology and Biological Psychiatry*. 2017;75:157-164.
588 doi:10.1016/j.pnpbp.2017.02.001

589 43. Zhang Z, Bo Q, Li F, et al. Increased ALFF and functional connectivity of the right
590 striatum in bipolar disorder patients. *Prog Neuropsychopharmacol Biol Psychiatry*.
591 2021;111:110140. doi:10.1016/j.pnpbp.2020.110140

592 44. Gong J, Wang J, Qiu S, et al. Common and distinct patterns of intrinsic brain activity
593 alterations in major depression and bipolar disorder: voxel-based meta-analysis.
594 *Transl Psychiatry*. 2020;10(1):353. doi:10.1038/s41398-020-01036-5

595 45. Tenev A, Markovska-Simoska S, Müller A, Mishkovski I. Entropy, complexity, and
596 spectral features of EEG signals in autism and typical development: a quantitative
597 approach. *Front Psychiatry*. 2025;16. doi:10.3389/fpsyt.2025.1505297

598 46. Menon V. Large-scale brain networks and psychopathology: a unifying triple network
599 model. *Trends Cogn Sci*. 2011;15(10):483-506. doi:10.1016/j.tics.2011.08.003

600 47. Foster ML, Ye J, Powers AR, Dvornek NC, Scheinost D. Connectome-based
601 predictive modeling of early and chronic psychosis symptoms.
602 *Neuropsychopharmacol*. Published online February 27, 2025:1-9.
603 doi:10.1038/s41386-025-02064-9

604 48. Schilbach L, Hoffstaedter F, Müller V, et al. Transdiagnostic commonalities and
605 differences in resting state functional connectivity of the default mode network in

schizophrenia and major depression. *NeuroImage: Clinical*. 2016;10:326-335. doi:10.1016/j.nicl.2015.11.021

49. COBRE Phase 3 | The Mind Research Network (MRN). Accessed February 14, 2025. https://www.mrn.org/common/cobre-phase-3

50. Lewandowski KE, Bouix S, Ongur D, Shenton ME. Neuroprogression across the Early Course of Psychosis. *J Psychiatr Brain Sci*. 2020;5:e200002. doi:10.20900/jpbs.20200002

51. Tanaka SC, Yamashita A, Yahata N, et al. A multi-site, multi-disorder resting-state magnetic resonance image database. *Sci Data*. 2021;8(1):227. doi:10.1038/s41597-021-01004-8

52. Gorgolewski KJ, Durnez J, Poldrack RA. Preprocessed Consortium for Neuropsychiatric Phenomics dataset. *F1000Res*. 2017;6:1262. doi:10.12688/f1000research.11964.2

53. American Psychiatric Association. *Diagnostic and Statistical Manual of Mental Disorders*. Fifth Edition. American Psychiatric Association; 2013. Accessed March 26, 2025. https://psychiatryonline.org/doi/book/10.1176/appi.books.9780890425596

54. Kay SR, Fiszbein A, Opler LA. The positive and negative syndrome scale (PANSS) for schizophrenia. *Schizophr Bull*. 1987;13(2):261-276. doi:10.1093/schbul/13.2.261

55. Beck AT, Ward CH, Mendelson M, Mock J, Erbaugh J. An inventory for measuring depression. *Arch Gen Psychiatry*. 1961;4:561-571. doi:10.1001/archpsyc.1961.01710120031004

56. Beck AT, Steer RA, Carbin MG. Psychometric properties of the Beck Depression Inventory: Twenty-five years of evaluation. *Clinical Psychology Review*. 1988;8(1):77-100. doi:10.1016/0272-7358(88)90050-5

57. Gorgolewski KJ, Durnez J, Poldrack RA. Preprocessed Consortium for Neuropsychiatric Phenomics dataset. *F1000Res*. 2017;6:1262. doi:10.12688/f1000research.11964.2

58. Shen X, Tokoglu F, Papademetris X, Constable RT. Groupwise whole-brain parcellation from resting-state fMRI data for network node identification. *Neuroimage*. 2013;82:403-415. doi:10.1016/j.neuroimage.2013.05.081

59. Shen X, Finn ES, Scheinost D, et al. Using connectome-based predictive modeling to predict individual behavior from brain connectivity. *Nat Protoc*. 2017;12(3):506-518. doi:10.1038/nprot.2016.178

60. Virtanen P, Gommers R, Oliphant TE, et al. SciPy 1.0: fundamental algorithms for scientific computing in Python. *Nat Methods*. 2020;17(3):261-272. doi:10.1038/s41592-019-0686-2

61. antropy.app_entropy — antropy 0.1.9 documentation. Accessed July 24, 2025. https://raphaelvallat.com/antropy/build/html/generated/antropy.app_entropy.html

62. Noble S, Mejia AF, Zalesky A, Scheinost D. Improving power in functional magnetic resonance imaging by moving beyond cluster-level inference. *Proceedings of the National Academy of Sciences*. 2022;119(32):e2203020119. doi:10.1073/pnas.2203020119

63. Schöttner M, Bolton TAW, Patel J, Nahálka AT, Vieira S, Hagmann P. Exploring the latent structure of behavior using the Human Connectome Project's data. *Sci Rep*. 2023;13(1):713. doi:10.1038/s41598-022-27101-1

64. ComBat-seq: batch effect adjustment for RNA-seq count data | NAR Genomics and Bioinformatics | Oxford Academic. Accessed July 30, 2025. https://academic.oup.com/nargab/article/2/3/lqaa078/5909519

65. M Y, Ka L, Pa C, et al. Statistical harmonization corrects site effects in functional connectivity measurements from multi-site fMRI data. *Human brain mapping*. 2018;39(11). doi:10.1002/hbm.24241

66. Zheng R, Chen Y, Jiang Y, et al. Dynamic Altered Amplitude of Low-Frequency Fluctuations in Patients With Major Depressive Disorder. *Front Psychiatry*. 2021;12. doi:10.3389/fpsyt.2021.683610

67. Madre M, Canales-Rodríguez EJ, Fuentes-Claramonte P, et al. Structural abnormality in schizophrenia versus bipolar disorder: A whole brain cortical thickness, surface area, volume and gyrification analyses. *Neuroimage Clin*. 2019;25:102131. doi:10.1016/j.nicl.2019.102131

68. Matsumoto J, Fukunaga M, Miura K, et al. Cerebral cortical structural alteration patterns across four major psychiatric disorders in 5549 individuals. *Mol Psychiatry*. 2023;28(11):4915-4923. doi:10.1038/s41380-023-02224-7

69. Koshiyama D, Fukunaga M, Okada N, et al. White matter microstructural alterations across four major psychiatric disorders: mega-analysis study in 2937 individuals. *Mol Psychiatry*. 2020;25(4):883-895. doi:10.1038/s41380-019-0553-7

70. Song X, Hu X, Zhou S, et al. Association of specific frequency bands of functional MRI signal oscillations with motor symptoms and depression in Parkinson's disease. *Sci Rep*. 2015;5(1):16376. doi:10.1038/srep16376

71. Caplan JB, Madsen JR, Raghavachari S, Kahana MJ. Distinct Patterns of Brain Oscillations Underlie Two Basic Parameters of Human Maze Learning. *Journal of Neurophysiology*. 2001;86(1):368-380. doi:10.1152/jn.2001.86.1.368

72. Ries A, Hollander M, Glim S, Meng C, Sorg C, Wohlschläger A. Frequency-Dependent Spatial Distribution of Functional Hubs in the Human Brain and

Alterations in Major Depressive Disorder. *Front Hum Neurosci*. 2019;13:146. doi:10.3389/fnhum.2019.00146

73. Bonnefond M, Kastner S, Jensen O. Communication between Brain Areas Based on Nested Oscillations. *eNeuro*. 2017;4(2). doi:10.1523/ENEURO.0153-16.2017

74. Buzsáki G, Draguhn A. Neuronal oscillations in cortical networks. *Science*. 2004;304(5679):1926-1929. doi:10.1126/science.1099745

75. Motivation, emotion, and their inhibitory control mirrored in brain oscillations - PubMed. Accessed August 7, 2025. https://pubmed.ncbi.nlm.nih.gov/17145079/

76. Liu ZZ, Qu HJ, Tian ZL, et al. Reproducibility of frequency-dependent low frequency fluctuations in reaction time over time and across tasks. *PLOS ONE*. 2017;12(9):e0184476. doi:10.1371/journal.pone.0184476

77. Guo X, Li J, Su Q, et al. Transcriptional correlates of frequency-dependent brain functional activity associated with symptom severity in degenerative cervical myelopathy. *NeuroImage*. 2023;284:120451. doi:10.1016/j.neuroimage.2023.120451

78. Buckley PF, Miller BJ, Lehrer DS, Castle DJ. Psychiatric Comorbidities and Schizophrenia. *Schizophr Bull*. 2009;35(2):383-402. doi:10.1093/schbul/sbn135

79. Kim S, Baek JH, Shim S hoon, et al. Alteration of cortical functional networks in mood disorders with resting-state electroencephalography. *Sci Rep*. 2022;12(1):5920. doi:10.1038/s41598-022-10038-w

80. Wang D, Peng X, Pelletier-Baldelli A, et al. Altered temporal, but intact spatial, features of transient network dynamics in psychosis. *Mol Psychiatry*. 2021;26(6):2493-2503. doi:10.1038/s41380-020-00983-1

81. Segal A, Parkes L, Aquino K, et al. Regional, circuit and network heterogeneity of brain abnormalities in psychiatric disorders. *Nat Neurosci*. 2023;26(9):1613-1629. doi:10.1038/s41593-023-01404-6

82. Helakari H, Kananen J, Huotari N, et al. Spectral entropy indicates electrophysiological and hemodynamic changes in drug-resistant epilepsy – A multimodal MREG study. *NeuroImage: Clinical*. 2019;22:101763. doi:10.1016/j.nicl.2019.101763

83. Yang GJ, Murray JD, Repovs G, et al. Altered global brain signal in schizophrenia. *Proceedings of the National Academy of Sciences*. 2014;111(20):7438-7443. doi:10.1073/pnas.1405289111

84. Bachiller A, Lubeiro A, Díez Á, et al. Decreased entropy modulation of EEG response to novelty and relevance in schizophrenia during a P300 task. *Eur Arch Psychiatry Clin Neurosci*. 2015;265(6):525-535. doi:10.1007/s00406-014-0525-5

85. Akar SA, Kara S, Latifoğlu F, Bilgiç V. Analysis of the Complexity Measures in the EEG of Schizophrenia Patients. *International Journal of Neural Systems*. Published online February 21, 2016. doi:10.1142/S0129065716500088

86. Karanikolaou M, Limanowski J, Northoff G. Does temporal irregularity drive prediction failure in schizophrenia? temporal modelling of ERPs. *Schizophr*. 2022;8(1):23. doi:10.1038/s41537-022-00239-7

87. Poza J, Hornero R, Abásolo D, Fernández A, Escudero J. Analysis of spontaneous MEG activity in patients with Alzheimer's disease using spectral entropies. *Annu Int Conf IEEE Eng Med Biol Soc*. 2007;2007:6180-6183. doi:10.1109/IEMBS.2007.4353766

88. Gómez C, Hornero R. Entropy and Complexity Analyses in Alzheimer's Disease: An MEG Study. *Open Biomed Eng J*. 2010;4:223-235. doi:10.2174/1874120701004010223

89. Ferdinando H, Moradi S, Korhonen V, Helakari H, Kiviniemi V, Myllylä T. Spectral entropy provides separation between Alzheimer's disease patients and controls: a study of fNIRS. *Eur Phys J Spec Top*. 2023;232(5):655-662. doi:10.1140/epjs/s11734-022-00753-w

90. McGrath JJ, Lim CCW, Plana-Ripoll O, et al. Comorbidity within mental disorders: a comprehensive analysis based on 145 990 survey respondents from 27 countries. *Epidemiol Psychiatr Sci*. 2020;29:e153. doi:10.1017/S2045796020000633

91. Hu L, Chen H, Su W, et al. Aberrant static and dynamic functional connectivity of the executive control network in lung cancer patients after chemotherapy: a longitudinal fMRI study. *Brain Imaging and Behavior*. 2020;14(3):927-940. doi:10.1007/s11682-020-00287-6

TABLES: MAIN ANALYSIS

Demographic Variable		Controls	Mood	Psychosis	Test Statistic
Sample Size		535	228	318	N/A
Age (years)		39.89 ± 15.3	38.31 ± 12.56	29.8 ± 13.21	W=75.48, df=2, p<0.001
Motion Frame Displacement (mm)		0.083 ± 0.046	0.087 ± 0.045	0.075 ± 0.037	W= 8.599, df=2, p=0.014
Dataset sample contributions		COBRE = 58 SRPBS = 281 HCP-EP = 57 UCLA = 117	COBRE = 0 SRPBS = 182 HCP-EP = 0 UCLA = 46	COBRE = 41 SRPBS = 124 HCP-EP = 112 UCLA = 41	N/A
Self-reported sex (n=1081, F/M)		272/263	79/149	135/183	χ^2=18.081, df = 2, p<0.001
BDI-II (n=62)		6.83 ± 6.39 (n=23)	22.13 ± 12.17 (n=39)	N/A	F=3.31; df=1, p<0.01
PANSS* (n=230)	Positive	N/A	N/A	10.96 ± 3.81	N/A
	Negative	N/A	N/A	13.98 ± 5.5	N/A
	General Psychopathology	N/A	N/A	24.63 ± 5.34	N/A
	Total	N/A	N/A	49.57 ± 10.93	N/A

Table 1: Descriptive Statistics of Participant Demographics by Clinical Group. Descriptive statistics of key demographic variables from the open-source datasets used in this study, including sex, motion, age, motion, and symptom score summaries. F=female; M=male. N/A = not applicable. PANSS=Positive and Negative Syndrome Scale, BDI-II =Beck's Depression Inventory. n=1081.

Scale	n	Clinical Group			Wilcoxon Rank Pairwise p		
		Control	Mood	Psychosis	C vs M	C vs P	M vs P
Whole-brain	823	0.008 ± 0.021	0.01 ± 0.019	-0.014 ± 0.039	p = 0.543 q = 0.543	**p = 7.16e-15 q = 2.15e-14**	**p = 8.04e-11 q = 1.21e-10**
Medial Frontal	846	0.008 ± 0.025	0.011 ± 0.025	-0.015 ± 0.041	p = 0.221 q = 0.221	**p = 3.79e-13 q = 1.14e-12**	**p = 6.56e-11 q = 9.84e-11**
Frontoparietal	852	0.007 ± 0.022	0.009 ± 0.022	-0.013 ± 0.04	p = 0.195 q = 0.195	**p = 6.08e-12 q = 1.82e-11**	**p = 2.53e-10 q = 3.79e-10**
Default Mode	882	0.008 ± 0.026	0.011 ± 0.025	-0.015 ± 0.046	p = 0.126 q = 0.126	**p = 2.23e-11 q = 6.7e-11**	**p = 1.98e-10 q = 2.97e-10**
Motor	881	0.008 ± 0.025	0.011 ± 0.024	-0.015 ± 0.042	p = 0.282 q = 0.282	**p = 2.34e-14 q = 7.01e-14**	**p = 1.01e-11 q = 1.51e-11**
Visual I	1081	0.004 ± 0.028	0.008 ± 0.029	-0.013 ± 0.044	p = 0.0807 q = 0.0807	**p = 4.3e-07 q = 6.45e-07**	**p = 9.31e-08 q = 2.79e-07**
Visual II	953	0.006 ± 0.03	0.007 ± 0.031	-0.013 ± 0.045	p = 0.722 q = 0.722	**p = 2.09e-09 q = 6.27e-09**	**p = 3.79e-07 q = 5.69e-07**
Visual Association	906	0.008 ± 0.025	0.01 ± 0.029	-0.016 ± 0.045	p = 0.184 q = 0.184	**p = 1.66e-13 q = 4.99e-13**	**p = 3.61e-11 q = 5.42e-11**
Salience	936	0.006 ± 0.024	0.009 ± 0.025	-0.014 ± 0.04	p = 0.171 q = 0.171	**p = 2.69e-12 q = 8.06e-12**	**p = 7.49e-12 q = 1.12e-11**
Subcortical	906	0.007 ± 0.025	0.011 ± 0.028	-0.016 ± 0.042	p = 0.328 q = 0.328	**p = 3.26e-14 q = 9.78e-14**	**p = 1.03e-11 q = 1.54e-11**
Cerebellar	823	0.011 ± 0.032	0.011 ± 0.029	-0.017 ± 0.053	p = 0.685 q = 0.685	**p = 5.69e-13 q = 1.71e-12**	**p = 6.62e-08 q = 9.93e-08**

Table 2. *Amplitude of low-frequency (ALFF, 0.01-0.08 Hz) value distributions by whole-brain, network and clinical group.* Reported values have had covariates linearly regressed and undergone site harmonization. n=sample size. Bolded table entries represent significant comparisons.

Scale	n	Clinical Groups (median +/- std)			Wilcoxon Rank Pairwise p		
		Control	Mood	Psychosis	C vs M	C vs P	M vs P
Whole-brain	823	-0.006 ± 0.012	0 ± 0.015	0.006 ± 0.023	**p = 2.14e-05 q = 3.21e-05**	**p = 1.39e-13 q = 4.18e-13**	p = 0.118 q = 0.118
Medial Frontal	846	-0.006 ± 0.014	-0.002 ± 0.015	0.008 ± 0.027	**p = 0.00523 q = 0.00523**	**p = 3.39e-13 q = 1.02e-12**	**p = 0.00522 q = 0.00523**
Frontoparietal	853	-0.005 ± 0.014	-0.001 ± 0.018	0.007 ± 0.025	**p = 0.00145 q = 0.00218**	**p = 1.7e-10, q = 5.09e-10**	**p = 0.0327 q = 0.0327**
Default Mode	882	-0.004 ± 0.016	-0.004 ± 0.019	0.007 ± 0.03	p = 0.218 q = 0.218	**p = 5.77e-08 q = 1.73e-07**	**p = 0.0016 q = 0.00241**
Motor	881	-0.006 ± 0.014	-0.003 ± 0.019	0.008 ± 0.027	**p = 0.00583 q = 0.00631**	**p = 1.98e-11 q = 5.94e-11**	**p = 0.00631 q = 0.00631**
Visual I	1081	-0.002 ± 0.017	-0.009 ± 0.03	0.009 ± 0.026	p = 0.0668 q = 0.0668	**p = 3.01e-09 q = 4.52e-09**	**p = 1.94e-09 q = 4.52e-09**
Visual II	954	-0.003 ± 0.018	-0.004 ± 0.027	0.007 ± 0.027	p = 0.177 q = 0.177	**p = 1.07e-08 q = 3.21e-08**	**p = 0.000637 q = 0.000955**
Visual Association	906	-0.005 ± 0.016	-0.006 ± 0.027	0.01 ± 0.028	p = 0.151 q = 0.151	**p = 1.92e-13 q = 5.76e-13**	**p = 3.56e-05 q = 5.35e-05**
Salience	846	-0.004 ± 0.013	-0.004 ± 0.021	0.009 ± 0.026	p = 0.0825 q = 0.0825	**p = 3.32e-10 q = 9.96e-10**	**p = 0.000402 q = 0.000603**
Subcortical	853	-0.005 ± 0.013	-0.005 ± 0.026	0.009 ± 0.026	**p = 0.00239 q = 0.00358**	**p = 5.29e-13 q = 1.59e-12**	**p = 0.0166 q = 0.0166**
Cerebellar	882	-0.007 ± 0.019	0.002 ± 0.019	0.007 ± 0.034	**p = 7.93e-06 q = 1.19e-05**	**p = 1.38e-08 q = 4.14e-08**	p = 0.544 q = 0.544

Table 3. *Low-frequency spectral entropy (lfSE, 0.01-0.08 Hz) value distributions by whole-brain, network and clinical group*. Reported values have had covariates linearly regressed and undergone site harmonization. n=sample size. Bolded table entries represent significant comparisons.

FIGURE HEADINGS

Figure 1. *Schematic of analysis pipeline at node and network levels*. This figure illustrates the study design and measurement calculation process. Four large-scale datasets were used in this study. A) First, the power spectrums were taken from preprocessed node-wise data, and the two low-frequency measures were calculated. Then, covariate regression of nuisance variables such as age, mean frame displacement, and sex were regressed using a generalized linear model. Where relevant, harmonization was performed to account for site effects. Then, the appropriate means were calculated for whole-brain (average over all nodes) and network (average over all member network nodes were taken for each of the 10 functional networks) analyses. B) Finally, group differences and symptom associations at whole-brain and network levels were calculated. FFT=Fast Fourier transform, ALFF=Amplitude of Low-Frequency Fluctuation, lfSE=low-frequency spectral entropy. $\bar{x}$=mean.

Figure 2. *Group Differences at Whole-brain Level and Symptom Associations.* Panels A and B feature a violin plot of the results for ALFF and lfSE respectively. Dots represent the participants (n=823; controls=366, mood=139, psychosis=318), colors represent the groups (controls, mood, psychosis). Panels C-E depict significant ALFF and lfSE symptom associations. Dots represent participants with a symptom score. A) Psychosis disorders had significantly lower ALFF than controls and mood disorders. B) Controls had significantly lower lfSE than mood and psychosis disorders. C) Significant BDI-II symptom associations with whole-brain ALFF (n=62). D) Significant positive PANSS symptom associations with whole-brain lfSE (n=230). E) Significant BDI-II symptom associations with whole-brain lfSE (n=62).

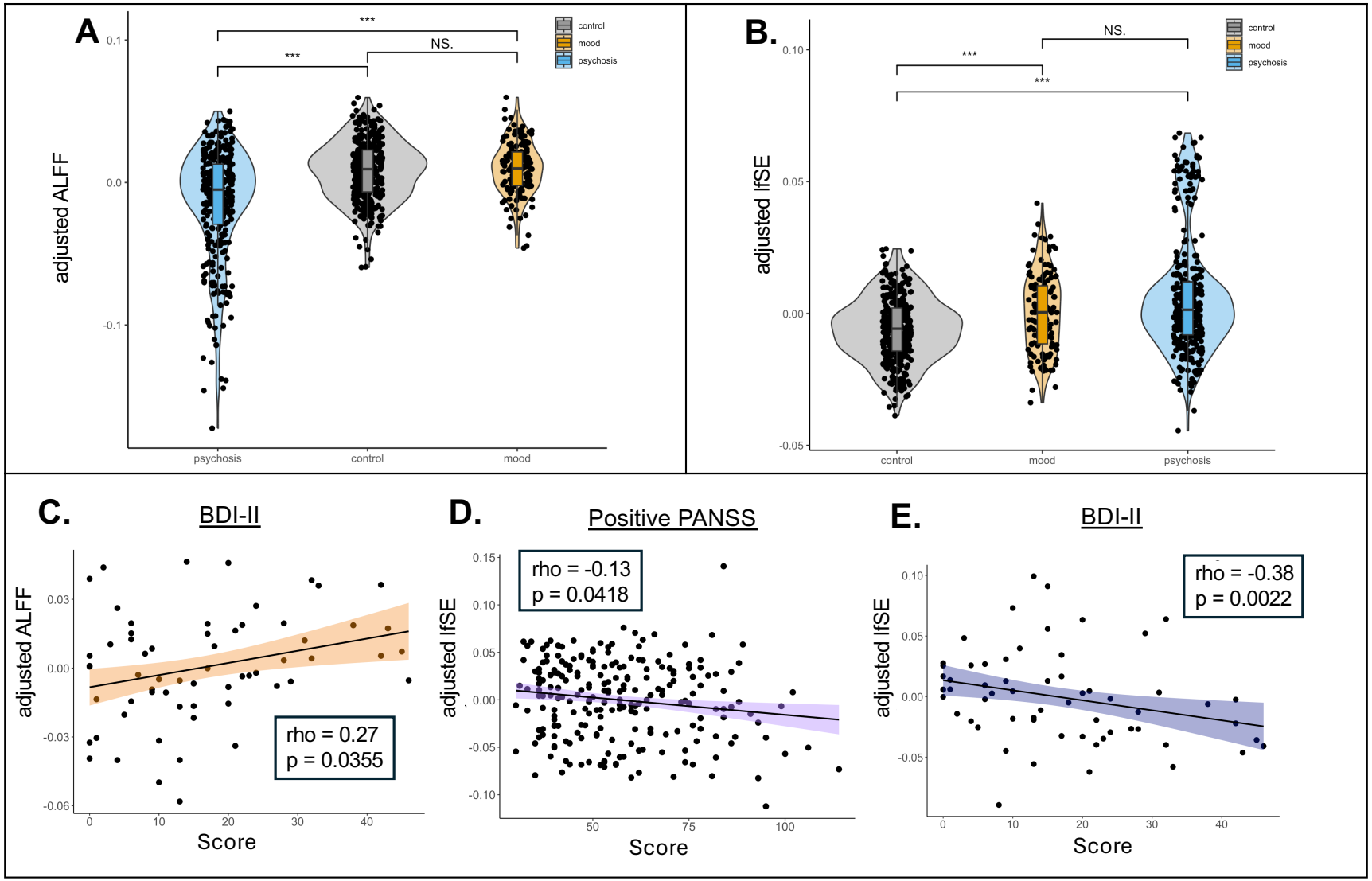
A
adjusted ALFF
0.1
0.0
-0.1
***
***
NS.
control
mood
psychosis
psychosis
control
mood
B.
adjusted lfSE
0.10
0.05
0.00
-0.05
***
***
NS.
control
mood
psychosis
control
mood
psychosis
C.
BDI-II
adjusted ALFF
0.03
0.00
-0.03
-0.06
rho = 0.27
p = 0.0355
0
10
20
30
40
Score
D.
Positive PANSS
adjusted lfSE
0.15
0.10
0.05
0.00
-0.05
-0.10
rho = -0.13
p = 0.0418
50
75
100
Score
E.
BDI-II
adjusted lfSE
0.10
0.05
0.00
-0.05
rho = -0.38
p = 0.0022
0
10
20
30
40
Score

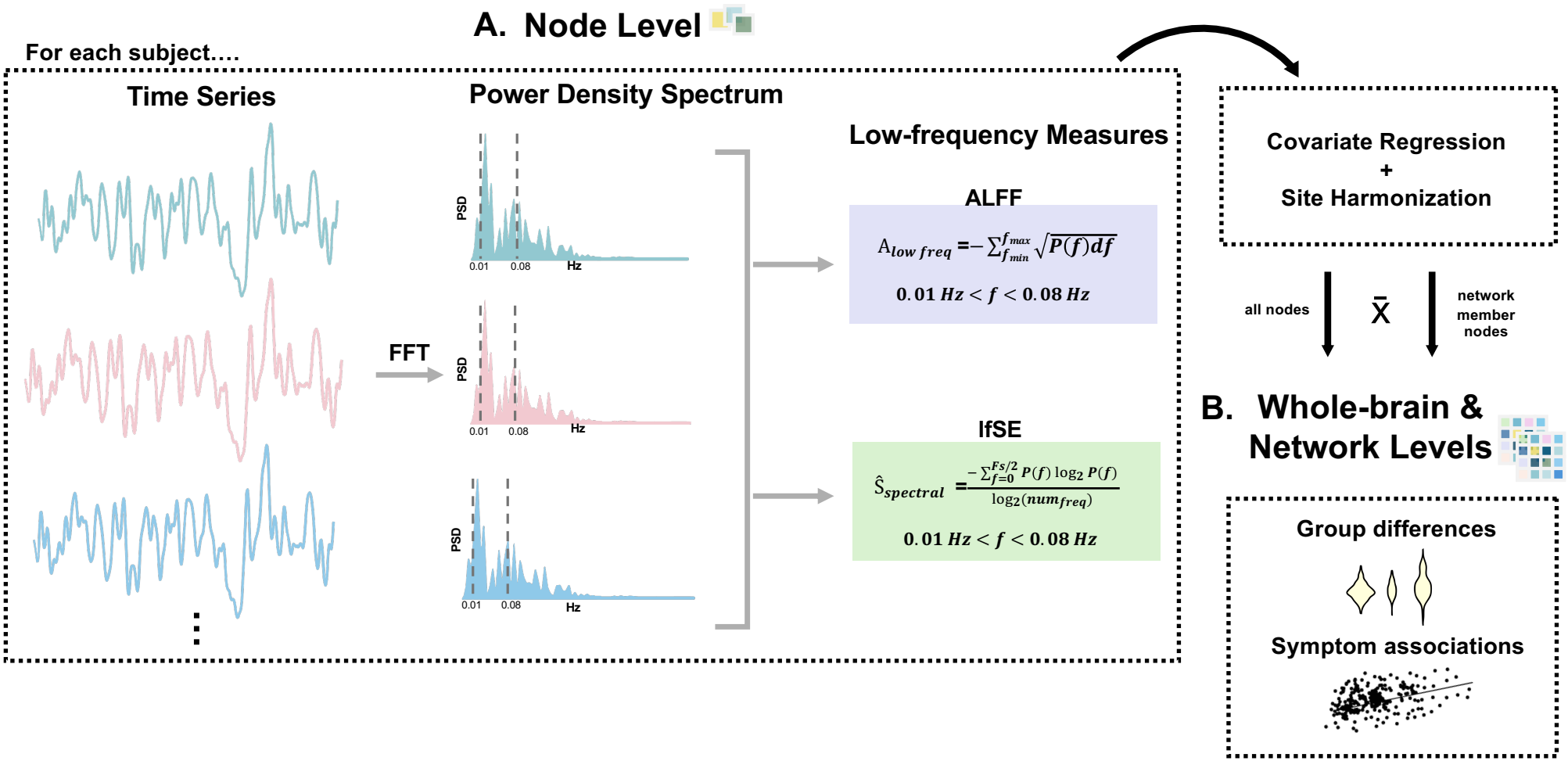
A. Node Level
For each subject….
Time Series
Power Density Spectrum
FFT
PSD
0.01
0.08
Hz
Low-frequency Measures
ALFF
$A_{low\ freq} = -\sum_{f_{min}}^{f_{max}} \sqrt{P(f)df}$
$0.01\ Hz < f < 0.08\ Hz$
IfSE
$\hat{S}_{spectral} = \frac{-\sum_{f=0}^{Fs/2} P(f)\log_2 P(f)}{\log_2(num_{freq})}$
$0.01\ Hz < f < 0.08\ Hz$
Covariate Regression
+
Site Harmonization
all nodes
$\bar{X}$
network member nodes
B. Whole-brain & Network Levels
Group differences
Symptom associations